

Can the Elliptic Billiard Still Surprise Us?

Dan Reznik · Ronaldo Garcia · Jair Koiller

Received: date / Accepted: date

Abstract Experimentation with $N = 3$ closed trajectories in Elliptic Billiards surprised us with new properties and invariants. Some have been subsequently proven and generalized for all N .

Keywords elliptic billiard, triangular orbits, elliptic loci

MSC 51M04 37D50 51N2051N3568T20

1 Introduction

Things in motion sooner catch the eye
Than what not stirs. –W.S., “Troilus and Cressida”

The venerable *Elliptic Billiard* (EB) has fascinated many a mathematician. It consists of a particle moving along a straight line in the interior of an ellipse, bouncing elastically against the boundary, Figure 1. This object has been exhaustively studied [25, 4]. But can it still yield any surprises?

Here is one. In 2011, we uploaded a [video](#) [15] showing the family of closed 3-periodic *orbits* in an EB. Since these are triangles, we also drew the locus of the Incenter and *Intouchpoints* (tangencies of Incircle with a triangle’s sides). The former was perfectly elliptic while the latter yields a self-intersecting sextic, Figure 2. Figure 3 provides a refresher on triangle concepts used here.

Over the next few years there surfaced elegant proofs showing that the locus of the Incenter [22, 6], Barycenter [24, 7], Circumcenter [5, 7], and Orthocenter [7] were all elliptic. In turn, this ushered us, some eight years later, into this second exploratory cycle. Indeed, the EB was chock-full of surprises!

D. Reznik
Upper West Soluções E-mail: dreznik@gmail.com

R. Garcia
Universidade Federal de Goiás E-mail: ragarcia@ufg.br

J. Koiller
Universidade Federal de Juiz de Fora E-mail: jairkoiller@gmail.com

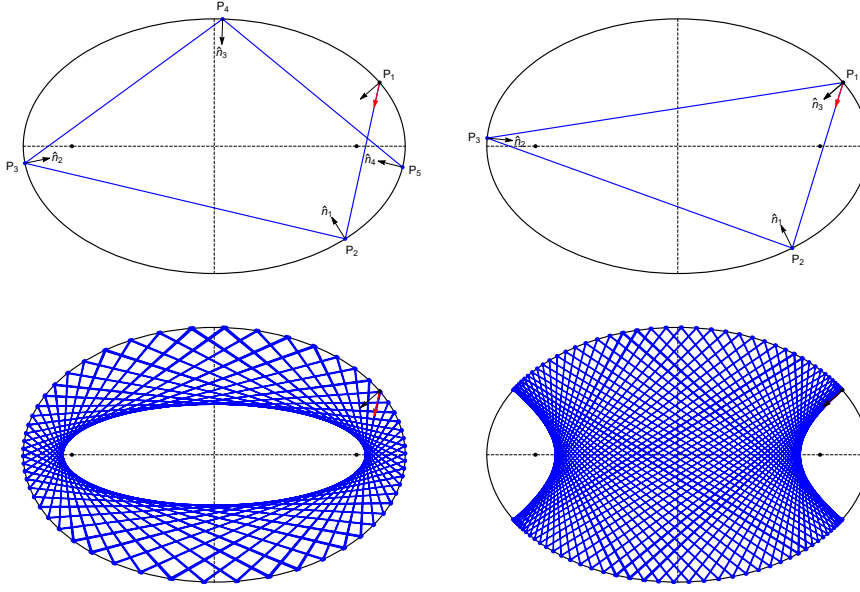


Fig. 1: Particle trajectories in an Elliptic Billiard. Top left: the first four segments of a trajectory starting at P_1 along the red arrow, bouncing elastically at P_2 , etc. Top right: a periodic trajectory with three edges. Bottom: quasi-periodic regimes tangent to an elliptic (left) or hyperbolic (right) *caustic*. [Video](#)

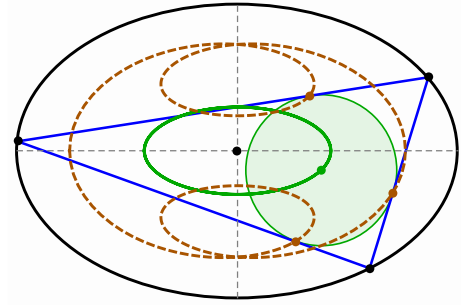


Fig. 2: An $N = 3$ orbit (blue), its Incircle (transparent green), Incenter (green dot) and Intouch Points (brown dots). Over the $N = 3$ family, the Incenter locus is a perfect ellipse (green), while the Intouchpoints produce a self-intersecting sextic (dashed brown). [Video](#)

1.1 Our experimental approach

New insights sprung from interactive experimentation with an [applet](#) [16] readily available to the reader. Additionally, many of our experiments have been placed on a YouTube [playlist](#) [17], and most figures in this document provide links to a corresponding video.

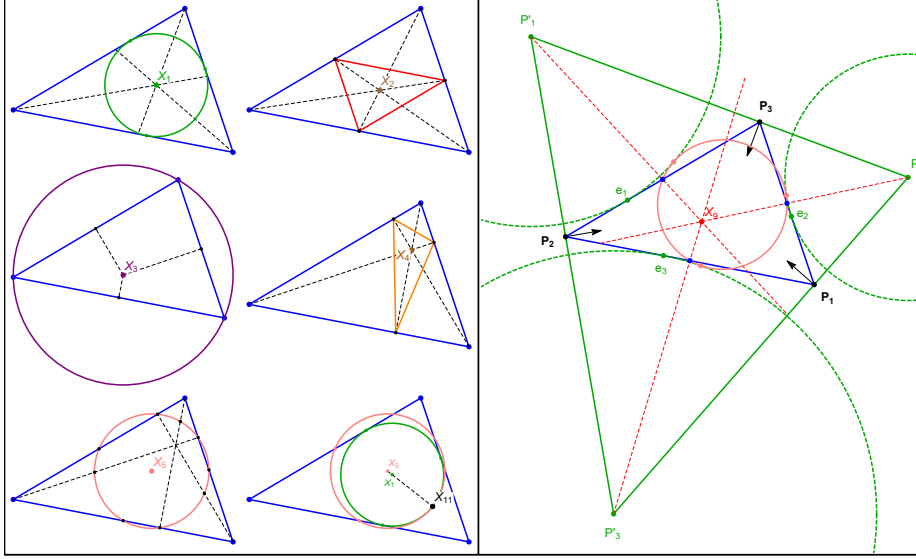


Fig. 3: Notable Triangle Points, referred to as X_i , after Kimberling [13]. **Left:** The Incenter X_1 is given by the intersection of angular bisectors. It is the center of the Incircle (green), tangent to the sides at three *Intouchpoints* (green dots), and its radius is the *Inradius* r . The Barycenter X_2 is the meet of lines drawn from the vertices to opposite sides' midpoints. The latter define the *Medial Triangle* (red). The Circumcenter X_3 is the intersection of perpendicular bisectors. This is the center of the *Circumcircle* (purple) whose radius is the *Circumradius* R . The Orthocenter X_4 is where the altitudes concur. Their feet form the *Orthic Triangle* (orange). X_5 is the center of the 9-Point (or Euler) Circle (pink): it passes through each side's midpoint, altitude feet, and Euler Points [29]. The Feuerbach Point X_{11} is the single point of contact between the Incircle and the 9-Point Circle. **Right:** given a reference triangle $P_1P_2P_3$ (blue), the *Excenters* $P'_1P'_2P'_3$ are pairwise intersections of lines through the P_i and perpendicular to the bisectors. This triad defines the *Excentral Triangle* (green). The *Excircles* (dashed green) are centered on the Excenters and are tangent to the triangle sides at the *Extouch Points* $e_i, i = 1, 2, 3$. Lines drawn from each Excenter through sides' midpoints (dashed red) concur at the *Mittenpunkt* X_9 . Also shown is Feuerbach's Theorem [29]: besides the Incircle, the 9-Pt Circle (pink) touches each Excircle at a single point (pink dots), the vertices of the *Feuerbach Triangle*.

We began by examining the loci of the first 100 *Triangle Centers* in Clark Kimberling's Encyclopedia¹ [13]. The curves we obtained included elliptic, circular, point-like, non-elliptic, quasi-elliptic, and with kinks [19]. Some of the elliptic ones were similar or even identical to the Billiard or its caustic.

Beyond loci, the $N = 3$ family revealed an amazing property: the ratio of Inradius to Circumradius is invariant. In turn, this implies beautiful relations involving orbit angles and areas.

¹ More than 40,000 are listed there!

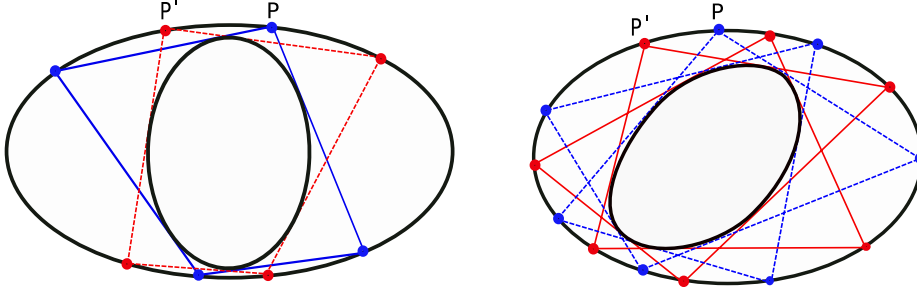


Fig. 4: Poncelet's Porism states that given two nested ellipses, if one closed trajectory with N sides can be found starting at a point P on the boundary of the outer, always remaining tangent to the inner, then every boundary point (e.g., P') can also initiate an N -trajectory, i.e., there exists a one-dimensional *family* of closed trajectories.

Close observation of the $N = 4$ family, associated with Monge's Orthoptic Circle [3], Figure 5, gave us clues with which to generalize $N = 3$ invariants to orbits of any N . These were also found to possess a point and a circular locus, and analogous angular and area invariants.

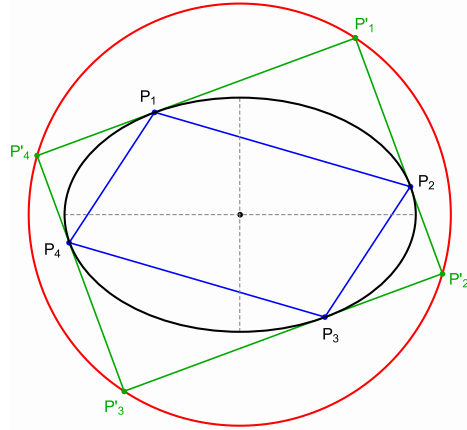


Fig. 5: French Mathematician Gaspard Monge (1746-1818) discovered that the locus of points whose tangents to a given ellipse subtend a right angle is a circle (red), called the *Orthoptic Circle*. Its connection with Billiards is direct: take a point P'_1 on the circle. Its tangents to the ellipse define a rectangle (green) on the circle whose tangents to the ellipse define a parallelogram (blue). This will also be a Billiard orbit of the ellipse! All $N = 4$ non-intersecting orbits are parallelograms. [Video](#)

Some proofs and insights herein have been privately contributed by generous mathematicians [23, 28, 27, 1, 9, 14], see Acknowledgements. We very much welcome reader feedback, including any help with questions we pose in the Conclusion.

2 Preliminaries: Integrability and Conservation

The most prominent property of an EB is its *Integrability* – the particle’s path can be expressed explicitly in terms of two Integrals of Motion: Energy and Joachimsthal’s [2, 25]. The EB is the only known integrable Billiard [12], and can be regarded as a special case of *Poncelet’s Porism* [4], Figure 4.

One first (and beautiful) consequence of integrability is that all N -orbits will have the same perimeter L [4]. A second one is that a quantity γ , related to Joachimsthal’s Integral, is also conserved. Consider an EB whose boundary satisfies $f(x, y) = (x/a)^2 + (y/b)^2 = 1$, then:

$$\gamma = \frac{1}{2} \nabla f(P) \cdot \hat{v} = \text{constant} > 0, \quad \forall P \quad (1)$$

where P is a vertex of the orbit, \hat{v} is the normalized incoming orbit vector and:

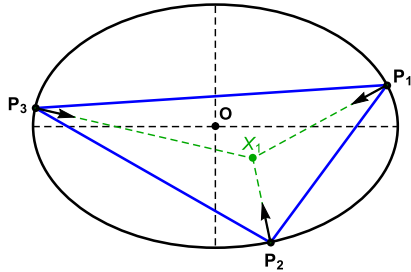
$$\nabla f = 2 \left(\frac{x}{a^2}, \frac{y}{b^2} \right)^t \quad (2)$$

For a given N , L and γ only depend on the Billiard axes a, b . Explicit expressions have been provided for $N = 3$ [7, 8]. Geometrically, the constancy of γ is equivalent to stating that all trajectory edges are tangent to a confocal ellipse, called the *caustic*, Figure 6b.

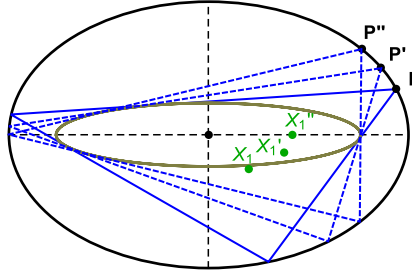
3 Locus Pocus: Curves Galore

3.1 Incenter Locus Recap

Consider an EB centered at O , and an $N = 3$ orbit, shown in Figure 6a. A vertex bisector is congruent with the inward normal to the ellipse, and these meet at the Incenter X_1 .



(a) An $N = 3$ orbit, and its Incenter X_1 : where the bisectors concur.



(b) Three triangular orbits, each identified by a starting vertex P, P', P'' , and their Incenters X_1, X_1', X_1'' , and the confocal caustic. [Video](#)

Fig. 6: Triangular Orbits in an EB and their Incenter.

Consider the three $N = 3$ orbits in Figure 6b, identified by a starting vertex P, P', P'' , as well as their Incenters X_1, X_1', X_1'' .

Though the Incenter's trilinear coordinates [29] are of the simplest form, $1 : 1 : 1$ [13], its Cartesian location will be non-linear on the vertices (explicit expressions are provided here [7]). This renders remarkable the following theorem, which we borrow from [22]:

Theorem 1 *The locus of the Incenter is elliptic.*

Also elliptic are the loci of the Barycenter X_2 , the Circumcenter X_3 , the Orthocenter X_4 [24, 5, 7]. Recently, this was also proven for the center X_5 of the 9-point circle [8], Figure 7b [18, video #1]. Indeed, numerical analysis of the first 100 Kimberling Centers (only 39,900 to go) reported that only 29 of them produce elliptic loci [8].

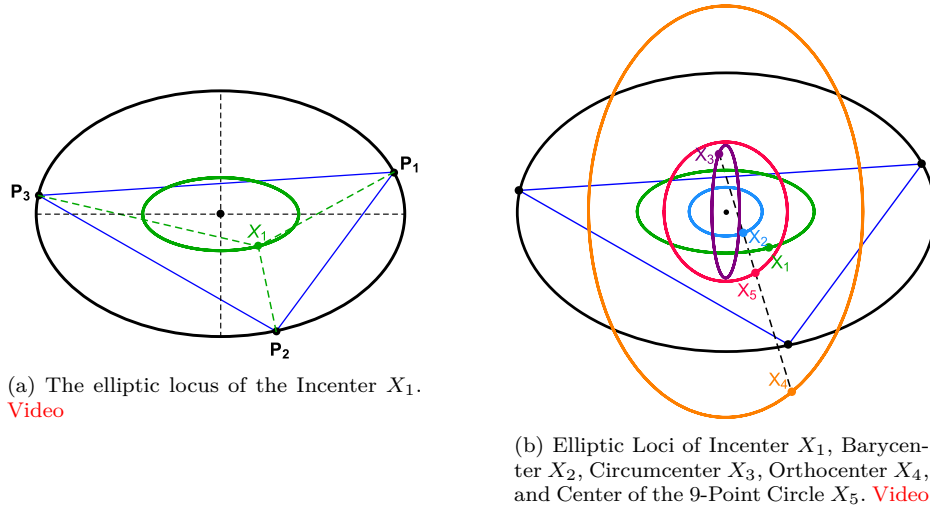


Fig. 7: Elliptic Loci of major triangle centers.

3.2 Eccentric Excenters

The *Excenters* are defined in Figure 3. In [7], Figure 8, the following is shown:

Theorem 2 *The locus of the Excenters is elliptic and similar to a rotated version of the Incenter's.*

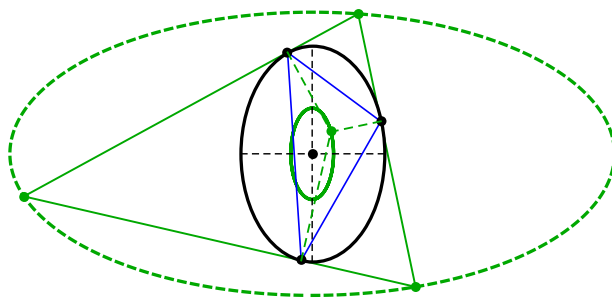


Fig. 8: An EB (black) is shown with its axes rotated (to save space), as well as an $N = 3$ orbit (blue) and its Excentral Triangle (solid green). The vertices of the Excentral Triangle move along an elliptic locus similar to a perpendicular copy of the Incircular locus (shown solid green inside the EB). [Video](#)

Though the vertices of the Excentral Triangle sweep an ellipse, consider those of the *Intouch Triangle*². As mentioned above, their locus is a self-intersecting sextic [15].

Generally, we've found that vertices of triangles derived from the orbit are non-elliptic. For example, vertices of the Feuerbach³ and Medial⁴ Triangles sweep non-elliptic curves, Figure 9. Surprisingly [8]:

Theorem 3 *The vertices of the Extouch Triangle, where Excircles touch the orbit sides, are not only elliptic, but congruent with the caustic.*

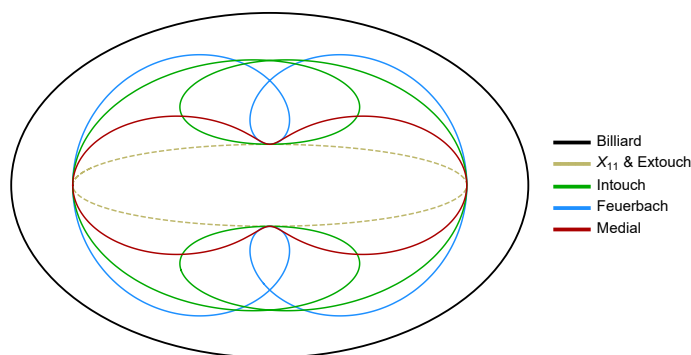


Fig. 9: The vertices of the Intouch (green), Feuerbach (blue), and Medial (red) Triangles sweep non-elliptic loci. Surprisingly, the Extouchpoints (as well as the Feuerbach Point X_{11}), sweep the $N = 3$ caustic. [Video](#)

² Points of contact of the Incircle with sides.

³ Points of contact of the 9-Pt Circle with the Excircles, Figure 3.

⁴ Triad of side midpoints

3.3 Fiery Feuerbach

The Feuerbach Point X_{11} is shown in Figure 3. Its *anticomplement*⁵ is called X_{100} . As depicted Figure 10, two surprising properties can be shown [8]:

Theorem 4 *The locus of X_{11} is congruent with the $N = 3$ caustic and the locus of X_{100} (its anticomplement) is congruent with the Billiard.*

We also noticed if orbit vertices slide along the Billiard in one direction, X_{11} (resp. the Extouchpoints) will sweep the caustic in the opposite (resp. same) direction as seen [here](#) [18, video #4].

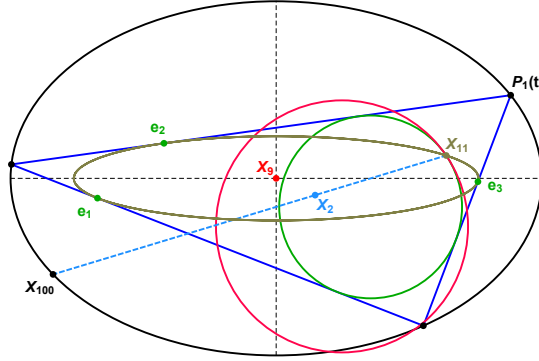


Fig. 10: The EB (black), as well as an $N = 3$ orbit (blue), with P_1 the starting vertex, and the caustic (brown). Also shown are the orbit's Incircle (green) and 9-Point Circle (pink), whose single point of contact is the Feuerbach Point X_{11} . Shown also is its anticomplement X_{100} , and the three Extouchpoints e_1, e_2, e_3 . Remarkable properties include: X_{11} and the Extouchpoints sweep the caustic, and X_{100} sweeps the Billiard (in opposite directions). [Video](#)

Other interesting locus phenomena were verified such as (i) the Symmedian Point⁶ X_6 is a convex quartic incredibly close to an ellipse (e.g., when $a/b = 1.5$), (ii) the orthic's incenter produces a locus with kinks ([Video](#)) (iii) the Intouchpoints of the Anticomplementary Triangle sweep the Billiard ([Video](#)). All of these can be interactively observed with our [applet](#).

4 A Point Locus

Triangular centers and derived vertices sweep out, we've seen, beautiful curves, elliptic or not. But one center, the *Mittenpunkt* X_9 , took us aback. As shown is Figure 11a and in [18, video #3]:

⁵ A point's double-length reflection about the barycenter X_2 .

⁶ Point of concurrence of a triangle's *symmedians*, i.e., the reflection of medians about the bisectors.

Theorem 5 *For an $N = 3$ orbit family, the Mittenpunkt X_9 is stationary at the Billiard's center.*

This fact can be proven by an affine transformation [23] explained in Figure 11c.

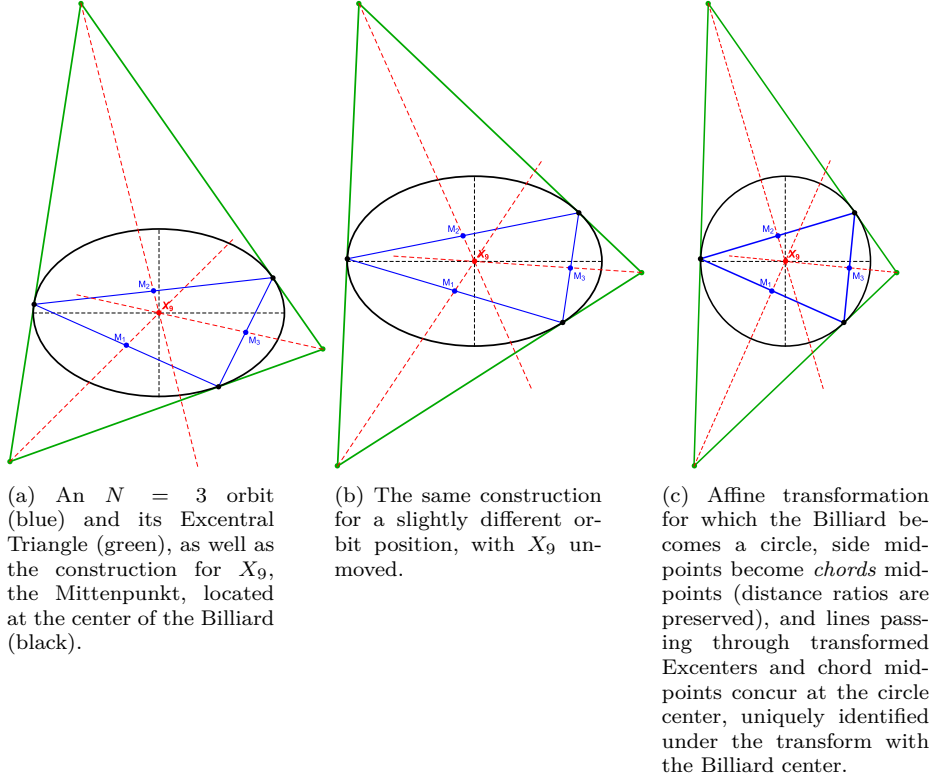


Fig. 11: Stationarity of X_9 and affine proof (pun intended!). [Video](#)

A triangle's *Circumellipse* [29] passes through its three vertices. For $N = 3$ orbits, we call this object a *Circumbilliard*. Since the orbit's Mittenpunkt X_9 is congruent with the Billiard's center, we can state ([Video](#)):

Corollary 1 *Every triangle has a circumellipse to which it is a Billiard orbit, whose center coincides with the triangle's Mittenpunkt.*

5 Constant Ratio of Radii

Denote the radii of an $N = 3$ orbit's Incircle, Circumcircle, and 9-Point Circle [29] as r (inradius) R (circumradius) and r_9 , respectively, Figure 12.

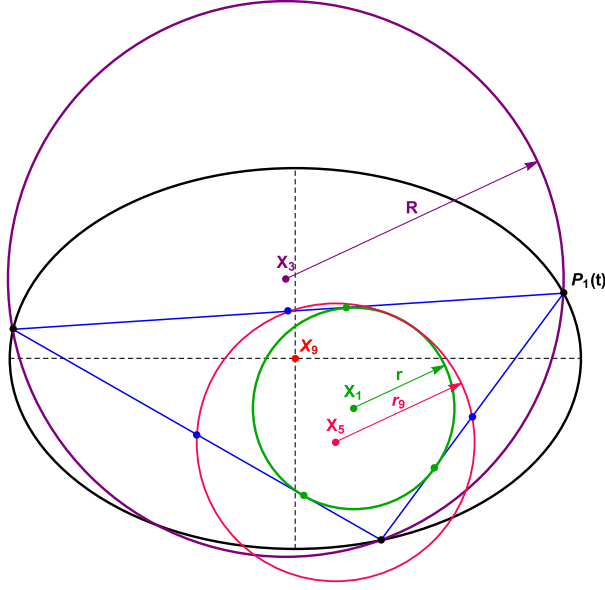


Fig. 12: An orbit (blue), a starting vertex P_1 , the Incircle (green), Circumcircle (purple), and 9-Point Circle (pink), whose centers are X_1 , X_3 , and X_5 , and radii are the inradius r , circumradius R , and 9-Point Circle radius r_9 . [Video](#)

The relation $R/r_9 = 2$ is well-known [29]. Remarkably [8]:

Theorem 6 *An $N = 3$ orbit family conserves the r/R ratio.*

Specifically, r/R can be expressed in terms of two known constants of motion: perimeter and angular momentum [14, 27], as follows:

$$\frac{r}{R} = \gamma L - 4 \quad (3)$$

Additionally, it can be shown that when the EB is circular, r/R is maximal at 0.5 (orbits are equilaterals). As $a/b \rightarrow \infty$, the ratio goes to zero.

5.1 Conservation of the Sum of Cosines

Denote $\theta_i, i = 1, 2, 3$ the angles internal to the orbit. The following is a remarkable identity valid for any triangle [11]:

$$\sum_{i=1}^3 \cos \theta_i = 1 + \frac{r}{R} \quad (4)$$

Since the right-hand side is constant, so must be the sum of the cosines! So a corollary to Theorem 6 is:

Corollary 2 *The $N = 3$ family conserves the sum of orbit cosines.*

5.2 Conservation of the Product of Excentral Cosines

A triangle is always the Orthic of its Excentral [29]. If θ'_i are the Excentral's angles, the following is a known relation [11]:

$$\prod_{i=1}^3 |\cos \theta'_i| = \frac{r}{4R} \quad (5)$$

Let θ'_i be an angle of the Excentral Triangle opposite to orbit angle θ_i . It can be shown that $\theta'_i = \frac{\pi - \theta_i}{2}$, i.e., the Excentral Triangle is acute. Therefore the absolute sign in Equation 5 can be dropped. Since the right hand side of the above is constant:

Corollary 3 *The $N = 3$ family conserves the product of Excentral cosines.*

A [video](#) was made to illustrate the simultaneous conservation of the sum of cosines by the $N = 3$ family and the product of cosines by the family's Excentral Triangles.

5.3 Conservation of Excentral-to-Orbit Area Ratio

Let A be the area of some triangle and A_h the area of its Orthic. A known relation is [11]:

$$\frac{A}{A_h} = \frac{2R_h}{r_h} \quad (6)$$

Since the orbit is its Excentral's Orthic, r/R constant implies:

Corollary 4 *The $N = 3$ family conserves the Excentral-to-Orbit area ratio.*

6 A Circular Locus

Loci can be elliptic, non-elliptic, or even a point. But can they be circular? And to boot, stationary? Let P be an $N = 3$ vertex and P' its reflection about the origin. By symmetry, this will “fall” on the Billiard. Let Q_1 and Q_2 be intersections of the tangent to the Billiard at P' with the orbit's Excentral Triangle T' . The following remarkable property is verified, illustrated in Figure 13a:

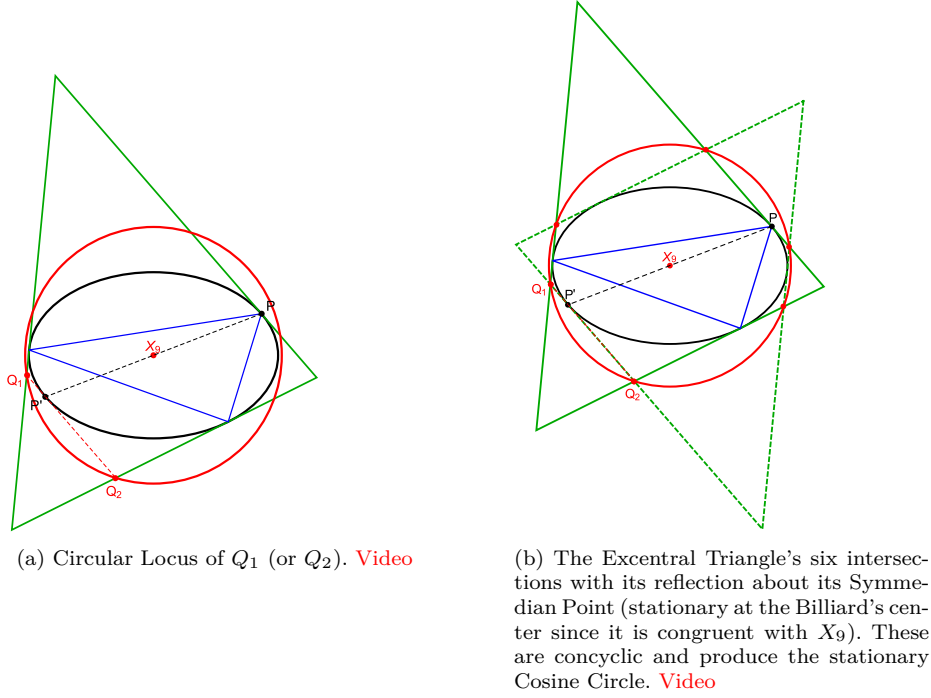


Fig. 13: Two construction of the Stationary Circular Locus. A third one (not shown) is based on six intersections of anti-parallel drawn through the Symmedian of the Excentral with the latter's sides – vertices of the *Cosine Hexagon* [29]. [Video](#)

Theorem 7 *The locus of Q_1 (or Q_2) is a stationary circle, and its center is the Billiard's.*

The circular locus is always external to the Billiard [8] and congruent with the *Cosine Circle* of the Excentral Triangle, also known as the *Second Lemoine Circle* [29]. Its center is the Symmedian Point of the Excentral. Since the latter is congruent with the orbit's Mittenpunkt, both radius and center are stationary.

The radius r^* of the stationary circle can be written as a function of the aspect ratio [8], or of constant perimeter and momentum [14, 27]:

$$r^* = \frac{L}{\frac{r}{R} + 4} = \frac{1}{\gamma} \quad (7)$$

No other *Tucker Circles* [29] for the $N = 3$ family have been found to be stationary. This surprising phenomenon can be viewed here [18, video #8].

7 Monge Madness: onward to $N > 3$

Close observation of the $N = 4$ orbit family, Figure 5, provided invaluable clues with which to generalize $N = 3$ invariants to $N > 3$ orbits. Namely:

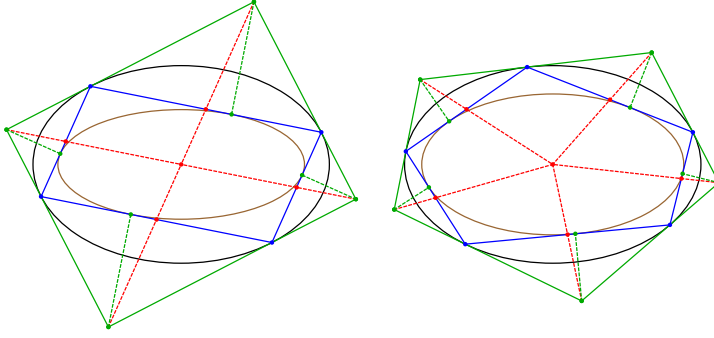


Fig. 14: Left: $N = 4$ (resp. Right: $N = 5$) orbits shown in blue. The dashed red lines connect vertices of the Tangential (green) to orbit sides' midpoints. Notice they intersect at the center of the Billiard, a type of generalized Mittenpunkt, [Video 1](#). Also shown are (dashed green) perpendiculars dropped from Tangential Vertices onto orbit sides. Their feet lie on and sweep the caustic (brown), [Video 2](#).

- Mittenpunkt: The lines connecting the Tangential Polygon's vertices to the parallelogram midpoints concur at the Ellipse's center.
- Null Sum of Cosines: The polygon formed by the four tangency points is a parallelogram therefore the sum of its cosines is zero.
- Null Product of Cosines: The Tangential Polygon is a rectangle and therefore the product of its cosines is zero.
- Stationary Circle: The orthoptic locus is a stationary circle.

7.1 $N > 3$ Stationary Point

For an $N = 3$ orbit, the Mittenpunkt is where lines drawn from each Excenter through the sides' midpoints meet. As shown in Figure 14, lines drawn from each vertex of the Tangential Polygon through the midpoint of the corresponding orbit side will meet at the stationary center of the Billiard [18, video #10]. The same proof via an Affine Transform used in Theorem 5, Figure 11c is used here, so we can state:

Theorem 8 *Given an $N \geq 3$ orbit family, the point of concurrence of lines drawn from tangential vertices through the midpoints of orbit sides is stationary at the center of the Billiard.*

7.2 Generalized Extouchpoints

Theorem 3 states Extouchpoints are on and sweep the $N = 3$ caustic. It turns out this is a special case of Chasles' Theorem [26]. Analogously, Figure 14:

Theorem 9 *The feet of perpendiculars dropped from vertices of the Tangential Polygon onto orbit sides are on the caustic and have the latter as their locus.*

This offers a method to easily “find” a point on the caustic which only requires two orbit vertices, as an alternate to [10] which required the Billiard's foci.

7.3 $N > 3$ Cosine Sum and Product

The fact that both $N = 3$ and $N = 4$ conserve cosine sum suggests $N > 4$ might as well, and this was first confirmed numerically for $N = 5, \dots, 30$ non-intersecting orbits at various Billiard aspect ratios. An elegant proof to this fact has been kindly contributed [28].

Theorem 10 *The sum of cosines is conserved for non-intersecting orbits, $\forall N$.*

Similarly, since both $N = 3$ and $N = 4$ conserve the product of their Excentral/Tangential cosines, we verify numerically that $N = 5, \dots, 30$ non-intersecting orbits at various aspect ratios also conserve this quantity. A proof to which (with similar techniques) has been kindly shared with us [1].

Theorem 11 *The product of cosines for the Tangential Polygon of non-intersecting orbits for any N is conserved.*

7.4 Area Ratio for $N > 3$

For $N = 3$ the Excentral-to-Orbit area ratio is conserved, however, we can numerically check this is not the case for $N = 4$. Proceeding to $N > 4$ we verify that only odd N preserve area ratio, a fact which has been subsequently formally proven [28].

Theorem 12 *The ratio of areas between Tangential Polygon and Non-Self-Intersecting Orbit is conserved for all odd N .*

7.5 Stationary $N > 4$ Circles

For the $N = 3$ case, Figure 13b, the locus of the intersection of an edge in the Excentral Triangle with an alternate edge reflected about the Billiard center is a stationary circle. For $N = 4$ we have Monge's Orthoptic Circle. Here is how these two constructions can be unified to $N > 4$, Figure 15, [18, video #9]:

Theorem 13 *Let O be the center of the Billiard. The locus of the intersection of an edge of the Tangential Polygon with the reflection of the next tangential edge about O is a stationary circle centered on O . Its radius is $r^* = 1/\gamma$.*

Proof Sketch [27]: Let ∇_X denote $\nabla f(X)$ as in Equation 2. Consider two consecutive vertices P and Q of the orbit. Momentum conservation (Equation 1) implies $\hat{v} \cdot \nabla_P = -\hat{v} \cdot \nabla_Q = 2\gamma$. So we have:

$$\hat{v} \cdot (\nabla_P + \nabla_Q) = 0 \quad (8)$$

Since ∇_P (resp. ∇_Q) is normal to the ellipse at P (resp. Q), a point z on the tangent line at P (resp. $-Q$) is given by $z \cdot \nabla_P = 2$ (resp. $z \cdot \nabla_Q = -2$). Let z be where both lines intersect, $z \cdot (\nabla_P + \nabla_Q) = 0$. It follows from Equation 8 that z is parallel to \hat{v} . Since $\hat{v} \cdot \nabla_P = 2\gamma$ and $z \cdot \nabla_P = 2$, we have $z = \hat{v}/\gamma$. That is, z lies on the circle of radius $1/\gamma$. \square

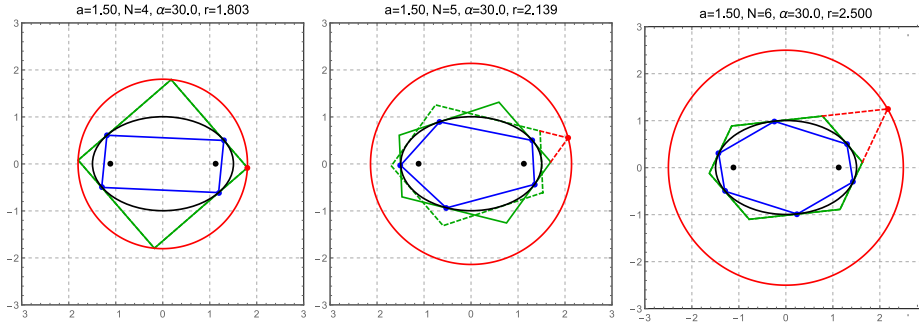


Fig. 15: The construction of a circular locus for $N = 4, 5, 6$. [Video 1](#) and [Video 2](#)

8 Conclusion & Questions

This second round of experiments with the Elliptic Billiard yielded many surprises, including interesting loci, a stationary point and circle, and conservation of radii ratios, angle sums, products, and area ratios. Many experimental results are available as online videos, images, and applets [20]. Further details are available in a companion website [21]. We leave the reader with a few questions:

- For $N = 3$, what determines whether a triangle center or derived vertex produces an elliptic vs some other type of locus?
- Are there ellipsoidal (3d) counterparts to these invariants?
- Which invariants are still true for self-intersecting orbits?
- Are there invariants for non-billiard (Poncelet) orbit families, e.g., created with two non-confocal or misaligned ellipses?
- Are there properties of triangle centers if orbits are defined on the unit sphere? Here edges become arcs of great circles (geodesics).

Acknowledgements We would like to thank Professors Sergei Tabachnikov, Richard Schwartz, Arseniy Akopyan, Olga Romaskevich, and Igor Minevich for invaluable mentoring, and key proofs. We would like to thank Profs. Jorge Zubelli, Marcos Craizer, Matt Perlmutter, and Ethan Cotterill, for inviting us for a talk at IMPA, PUC-RJ, UFF-RJ, and UFMG, respectively, and Paulo Ney de Souza for encouraging us to pursue this work and helping with the typesetting. We also thank Mark Helman for contributing proofs for the ellipticity of several triangular centers and Dominique Laurain for contributing (via Youtube!) a surprising expression for the radius of the Cosine Circle.

References

1. Akopyan, A.: Proofs of constant cosine product, and area ratio for $n > 3$. Private Communication (2019)
2. Birkhoff, G.: On the periodic motions of dynamical systems. *Acta Mathematica* **50**(1), 359–379 (1927). DOI 10.1007/BF02421325. URL <https://doi.org/10.1007/BF02421325>
3. Connes, A., Zagier, D.: A property of parallelograms inscribed in ellipses. *The American Mathematical Monthly* **114**(10), 909–914 (2007). URL <https://people.mpim-bonn.mpg.de/zagier/files/amm/114/fulltext.pdf>

4. Dragović, V., Radnović, M.: Poncelet Porisms and Beyond: Integrable Billiards, Hyperelliptic Jacobians and Pencils of Quadrics. *Frontiers in Mathematics*. Springer, Basel (2011). URL <https://books.google.com.br/books?id=QcOmDAEACAAJ>
5. Fierobe, C.: On the circumcenters of triangular orbits in elliptic billiard (2018). URL <https://arxiv.org/pdf/1807.11903.pdf>
6. Garcia, R.: Centers of inscribed circles in triangular orbits of an elliptic billiard (2016). URL <https://arxiv.org/pdf/1607.00179v1.pdf>
7. Garcia, R.: Elliptic billiards and ellipses associated to the 3-periodic orbits. *American Mathematical Monthly* **126**(06), 491–504 (2019). URL <https://doi.org/10.1080/00029890.2019.1593087>
8. Garcia, R., Reznik, D., Koiller, J.: New properties of triangular orbits in elliptic billiards (2019). In preparation
9. Helman, M.: The loci of $X_i, i = 7, 40, 57, 63, 142, 144$ are elliptic. Private Communication (2019)
10. Himmelstrand, M., Wilén, V., Saprykina, M.: A survey of dynamical billiards (2012). URL <https://pdfs.semanticscholar.org/3d98/090d1023f48be37d534682ad989a89cb0042.pdf>
11. Johnson, R.A.: *Modern Geometry: An Elementary Treatise on the Geometry of the Triangle and the Circle*. Houghton Mifflin, Boston, MA (1929)
12. Kaloshin, V., Sorrentino, A.: On the integrability of Birkhoff billiards. *Phil. Trans. R. Soc. A*(376) (2018). DOI <https://doi.org/10.1098/rsta.2017.0419>
13. Kimberling, C.: *Encyclopedia of triangle centers* (2019). URL <https://faculty.evansville.edu/ck6/encyclopedia/ETC.html>
14. Laurain, D.: Formula for the radius of the orbits' excentral cosine circle. Private Communication (2019)
15. Reznik, D.: Locus of the incircle touchpoints is a higher-order curve (2011). URL <https://youtu.be/9xU6T7hQMzs>
16. Reznik, D.: Applet showing the locus of several triangular centers (2019). URL <https://editor.p5js.org/dreznik/full/i1Lin7lt7>
17. Reznik, D.: Elliptic billiards playlist 2019 (2019). URL <https://bit.ly/2k5GXbB>
18. Reznik, D.: New properties of polygonal orbits in elliptic billiards: Main videos (2019). URL <https://bit.ly/2k5GXbB>
19. Reznik, D.: Triangular orbits in elliptic billiards: Loci of points $X(1)$ $X(100)$ (2019). URL https://dan-reznik.github.io/Elliptical-Billiards-Triangular-Orbits/loci_6tri.html
20. Reznik, D., Garcia, R., Koiller, J.: Media for elliptic billiards and family of orbits (2019). URL <https://dan-reznik.github.io/Elliptical-Billiards-Triangular-Orbits/videos.html>
21. Reznik, D., Garcia, R., Koiller, J.: New properties of triangular orbits in elliptic billiards (2019). URL <https://dan-reznik.github.io/Elliptical-Billiards-Triangular-Orbits/>
22. Romaskevich, O.: On the incenters of triangular orbits on elliptic billiards. *Enseign. Math.* **60**(3-4), 247–255 (2014). DOI 10.4171/LEM/60-3/4-2. URL <https://pdfs.semanticscholar.org/e0a4/4c62befebf56472cda62589dacbc404f8710.pdf>
23. Romaskevich, O.: Proof the mittenpunkt is stationary. Private Communication (2019)
24. Schwartz, R., Tabachnikov, S.: Centers of mass of Poncelet polygons, 200 years after. *Math. Intelligencer* **38**(2), 29–34 (2016). DOI 10.1007/s00283-016-9622-9. URL <http://www.math.psu.edu/tabachni/prints/Poncelet5.pdf>
25. Tabachnikov, S.: *Geometry and Billiards*, *Student Mathematical Library*, vol. 30. American Mathematical Society, Providence, RI (2005). DOI 10.1090/stml/030. URL <http://www.math.psu.edu/tabachni/Books/billiardsgeometry.pdf>. Mathematics Advanced Study Semesters, University Park, PA
26. Tabachnikov, S.: Projective configuration theorems: old wine into new wineskins. arXiv preprint arXiv:1607.04758 (2016)
27. Tabachnikov, S.: Proofs of stationary circle radius for $n > 3$. Private Communication (2019)
28. Tabachnikov, S., Schwartz, R.: Proof of constant cosine sum $n > 3$. Private Communication (2019)
29. Weisstein, E.: Mathworld (2019). URL <http://mathworld.wolfram.com>